ACS APPLIED MATERIALS & INTERFACES

www.acsami.org

Research Article

Self-Densified Optically Transparent VO_2 Thermochromic Wood Film for Smart Windows

Sai Liu, Chi Yan Tso,* Hau Him Lee, Yu Wei Du, Kin Man Yu, Shien-Ping Feng, and Baoling Huang

Cite This: https://doi.org/10.1021/acsami.1c03803

Read Online

ACCESS | Metrics & More | Article Recommendations | Supporting Information

ABSTRACT: Optically transparent wood has emerged as a promising glazing material. Thanks to the high optical transmittance, strong mechanical properties, and excellent thermal insulation capability of transparent wood, it offers a potential alternative to glass for window applications. Recently, thermo-, electro-, and photochromic transparent woods that dynamically modulate light transmittance have been investigated to improve building energy efficiency. However, it remains challenging to widely replace windows with transparent wood because of its poor weather resistance. In this study, an environment-friendly thermochromic transparent wood film (TTWF) with thermal switching of transmittance is proposed and demonstrated. To achieve thermochromism, the bleached wood is impregnated with the vanadium dioxide (VO_2)/polyvinyl alcohol composite. Due to the self-densification of cellulose microfibrils during the evaporation of solvents, the transparent wood is in the form of thin films, which can be attached on the inner face of a window to protect it from severe weather conditions, making the installation convenient and low-cost. Furthermore, the surface of VO_2-TTWF is modified by octadecyltrichlorosilane to enhance the waterproof ability and achieve self-cleaning and antidust functions. The proposed VO_2-TTWF shows great potential for application in energy-efficient buildings using sustainable materials with advanced optical properties (*i.e.*, T_{lum} = 50.5%, ΔT_{sol} = 3.4%, and haze = 70%) that are mechanically robust (*i.e.*, σ = 130.6 MPa along the wood growth direction), have low-thermal conductivity (*i.e.*, K = 0.29 W m^{-1} K^{-1} along the perpendicular direction to the wood fibers), and demonstrate hydrophobic self-cleaning and antidust functions (*i.e.*, contact angle: 121.9°). An experiment, using a model house, showed that the VO_2-TTWF attached on the inner face of the window could significantly reduce the indoor air temperature by 33.9 °C compared with a bare glass panel, proving that VO_2-TTWF has potential to be applied as a new-generation energy-efficient material for smart windows.

KEYWORDS: *energy-efficient glazing, thermochromic smart windows, transparent wood, thermal management, vanadium dioxide*

1. INTRODUCTION

Wood is a renewable and sustainable material which has been widely used in our daily life for items, such as furniture, decoration, and infrastructure.[1] The remarkable mechanical properties and low-thermal conductivity as well as the low density of wood attract the attention of researchers to develop various multifunctional wood-based materials.[2−5] Recently, newly developed transparent wood has attracted a lot of attention as an energy-saving material. Transparent wood is an optically transparent composite of delignified wood with matching polymers in terms of refractive index, such as epoxy,[6,7] polymethyl methacrylate (PMMA),[8] and polyvinylpyrrolidone.[9] Being transparent, it shows great potential to be an alternative material for traditional glass. Compared with single-pane glass windows, the intrinsic thermal conductivity of transparent wood is much lower, leading to excellent thermal insulation in buildings.[10] Moreover, transparent wood is not as fragile as glass, reducing the hazard of breaking upon sudden impact[11] and enhancing the safety. Most importantly, wood is a sustainable material, and the fabrication process of transparent wood is environmentally friendly compared with glass production which produces massive amounts of CO_2.[12]

Besides these advantages, transparent wood can be easily functionalized because of its intrinsic microchannels formed by a cellulose scaffold.[1] Yu *et al.* developed a heat-shielding transparent wood by infiltrating Cs_xWO_3/PMMA, which can block near-infrared (NIR) light for potential application in energy-efficient buildings.[13] Recently, Zhang *et al.* impregnated pine wood with epoxy resin and VO_2 and developed a thermally insulated transparent wood.[14] Additionally, a solar irradiation experiment was also built to investigate the infrared

Received: February 27, 2021
Accepted: April 28, 2021

thermal-shielding performance, showing that the transparent wood composite effectively reduced the indoor air temperature. Unfortunately, the solar modulation ability, one of the key parameters of thermochromism, is not reported in their study. On the other hand, Lang *et al.* developed an electrochromic transparent wood using poly(3,4-ethylenedioxy-thiophene)/poly(styrene sulfonate) (PEDOT/PSS) as an electrode. A magenta-to-clear transition behavior was exhibited by applying different voltages.[15] Wang *et al.* experimentally demonstrated a photochromic transparent wood by mixing 3′,3′-dimethyl-6-nitro-spiro[2*H*-1-benzopyran-2,2′-indoline]-1′-ethanol with PMMA. They reported that the photochromic transparent wood exhibited a photoresponse color-tuning ability in the visible-light region.[16] However, it should be noted that studies of optically regulated thermochromic transparent wood for application in windows are still rare. Compared with electrochromic and photochromic smart windows, thermochromic smart windows have certain advantages since they are (i) passive and require no electricity to power the change in optical transmittance;[17] (ii) low cost to manufacture and maintain due to the simple configuration;[18] and (iii) regulated by temperature instead of UV-triggered optical modulation.[19] They can replace conventional windows in buildings, vehicles, aircraft, and ships to save energy. Among different thermochromic materials, vanadium dioxide (VO_2) is widely investigated as it can modulate the transmittance of solar radiation because of its internal reversible phase change from a metal (hot state) to an insulator (cold state) at a critical-transition temperature of 68 °C.[20,21] The phase change gives rise to an abrupt change in the NIR transmittance so that VO_2 shows high transmittance in the NIR region at the cold state and becomes opaque to NIR light at the hot state. The solar energy in the NIR region accounts for around 49%, so the NIR regulation ability of VO_2 enables the window to save a lot of energy. In addition, the transition temperature of VO_2 can be modulated by doping with various metal ions. For example, by doping tungsten (W), the transition temperature of VO_2 can be reduced, close to room temperature.[22] Although a lot of research has been devoted to the study of various functional transparent woods, there is still a long way to go before they completely replace traditional windows, and one major concern is the poor durability of wood under extreme and changeable weather conditions (*e.g.*, heavy rains and windy days).

In this study, a self-densified VO_2 thermochromic transparent wood film (VO_2-TTWF) with thermo-switching of transmittance in the NIR region is proposed. It should be noted that the VO_2 thermochromic transparent wood developed in this work is made in the form of a film, implying that it can be easily and directly attached on the inner side of existing windows to reduce the installation cost and simultaneously avoid the weather resistance problem of wood, thereby extending its life span. Previous studies reported that polymer-based VO_2 materials were applied as coatings for smart windows,[23] but the mechanical strength of polymer-based VO_2 film needs to be further enhanced. Therefore, in this study, the VO_2−polymer mixture was integrated with a unique hierarchical structure of wood to develop a robust thermochromic wood film. To fabricate VO_2-TTWF, W-doped VO_2 nanoparticles are well dispersed in polyvinyl alcohol (PVA), which is then used to impregnate the lignin modified wood. Compared with other polymers (*e.g.* epoxy, PMMA), PVA is a rare polymer which is biodegradable under a natural environment.[24] This feature makes VO_2-TTWF truly sustainable, recyclable, and a green construction material. Besides, due to the rapid solvent evaporation of PVA solution during the polymerization process, the overall thickness of the transparent wood can be significantly reduced and the self-densification of cellulose microfibrils leads to a stronger hydrogen bonding between the PVA and cell walls, resulting in a robust wood film.[25] The proposed VO_2-TTWF demonstrates good properties in multiple aspects, namely, smart optical regulation ability (*i.e.*, T_{lum} = 50.5% & ΔT_{sol} = 3.4%, haze of 70%), strong mechanical properties (with a tensile strength of 130.6 MPa and a Young's modulus of 5.2 GPa), and a low-thermal conductivity (0.29 W m^{-1} K^{-1}). Furthermore, VO_2-TTWF is modified by coating with octadecyltrichlorosilane (OTS)[26] to achieve a hydrophobic surface for improving water resistance for window applications, while simultaneously achieving the self-cleaning and antidust functions (*i.e.*, the contact angle of VO_2-TTWF is 121.9°). Finally, an experimental test using model houses under the infrared (IR) lamp demonstrates that VO_2-TTWF can achieve significant indoor air temperature reduction by about 33.9 °C compared with a bare glass window. Overall, VO_2-TTWF shows great potential to be applied in energy-efficient buildings as the next-generation glazing technique.

2. EXPERIMENTAL SECTION

2.1. Delignification. Sodium hypochlorite solution (NaClO, available Cl ≥ 5%, Aladdin) is diluted to 5%, and the balsa wood slices (35 mm × 35 mm × 1 mm) are immersed in the NaClO solution for 12 h at room temperature. Next, the wood slices are rinsed with deionized water and ethanol. The slices are stored in a 96% ethanol solution at 4 °C for the next process.

2.2. Fabrication of the VO_2 Thermochromic Transparent Wood Film. VO_2 nanoparticles doped with W (concentration of W: 2 wt ‰; particle size: 30−50 nm) (Ji Kang New Material, China) are dispersed in 50 mL of DI water. The nanoparticles are weighed to be 4.35, 13.05, and 26.1 mg as nominal 1, 3, and 6 wt ‰ for samples with different VO_2 concentrations, respectively. The mixture is blended by a magnetic stirrer for 12 h, followed by an ultrasonic process to reduce the concentration of aggregated VO_2 nanoparticles. After that, 4.35 g of PVA (Sigma-Aldrich) is dissolved in the mixture at 90 °C. Hereafter, the delignified wood is impregnated with the PVA/VO_2 solution under the vacuum condition. The process is repeated five times to ensure full impregnation. Next, the wet wood is taken from the PVA solution and placed on a Petri dish. VO_2-TTWF can be tightly attached to the Petri dish because of the surface tension between VO_2-TTWF and the Petri dish. In this way, the curling problem can be avoided in the next solidification process. Finally, the wood is completely solidified in an oven at 60 °C, and the final product can be peeled off from the Petri dish.

2.3. Surface Treatment for Hydrophobicity. The aim of the following procedures is to achieve a hydrophobic surface on VO_2-TTWF for self-cleaning and antidust functions. First, 1 g of PVA is dissolved in 25 mL of DI water at 90 °C. 0.3 g of SiO_2 nanoparticles (DK Nano Technology, particle size: 30 nm) is well dispersed into the PVA solution by magnetic stirring (12 h) and an ultrasonic process (2 h). A small amount of mixture solution is dripped on VO_2-TTWF and dried at room temperature. Then, a 1.5:100 (V/V) OTS (J&K Chemical) *n*-hexane (Acros) solution is prepared, into which VO_2-TTWF is immersed for 2 h followed by drying in a hot oven at 40 °C, leading to the hydrophobic surface on VO_2-TTWF.

2.4. Characterization. The crystalline structure of W-doped VO_2 powders is characterized using X-ray diffraction (XRD) (PANalytical X'Pert^3 powder diffractometer). The transition temperature of VO_2 powders is measured by differential scanning calorimetry (DSC) (TA Q1000); the endothermic and exothermic peaks correspond to the transition temperature of heating and cooling processes of VO_2,

https://doi.org/10.1021/acsami.1c03803
ACS Appl. Mater. Interfaces XXXX, XXX, XXX−XXX

respectively. A ZEISS EVO MA10 scanning electron microscope (SEM) is used for characterizing the morphologies of the samples with a layer of gold sputtered on the sample surface (Quorum Technologies Q150T ES). The transmittance spectra of VO_2-TTWF under the cold and hot states are measured by a SHIMADZU UV3600 UV−vis−NIR spectrophotometer. There are two vital indices to quantify the optical performance of VO_2-TTWF, namely, the luminous transmittance (T_{lum}) and solar modulation ability (ΔT_{sol}).[18,21] T_{lum} is the amount of visible light transmitted by the VO_2-TTWF that is useful for human vision under normal conditions; it is defined as

$$T_{lum} = \frac{\int_{\lambda=380nm}^{780nm} \bar{y}(\lambda)T(\lambda)d\lambda}{\int_{\lambda=380nm}^{780nm} \bar{y}(\lambda)d\lambda} \quad (1)$$

where $T(\lambda)$ is the transmittance of the VO_2-TTWF at wavelength λ. $\bar{y}(\lambda)$ is the photopic luminous efficiency of the human eye defined by the CIE (International Commission on Illumination) standard. The wavelength range of 380−780 nm corresponds to the limits of human vision. The solar transmittance (T_{sol}) is the integral transmittance under AM 1.5 solar irradiation and is given by

$$T_{sol} = \frac{\int_{\lambda=300nm}^{2500nm} \text{AM } 1.5(\lambda)T(\lambda)d\lambda}{\int_{\lambda=300nm}^{2500nm} \text{AM } 1.5(\lambda)d\lambda} \quad (2)$$

The solar modulation ability (ΔT_{sol}) of a VO_2-TTWF is the solar transmittance between cold ($T_{sol,cold}$) and hot ($T_{sol,hot}$) states, which is calculated as

$$\Delta T_{sol} = T_{sol,cold} - T_{sol,hot} \quad (3)$$

The calculation of haze based on ASTM D1003 "Standard Method for Haze and Luminous Transmittance of Transparent Plastics"[8] is defined as

$$\text{haze} = \left(\frac{T_4}{T_2} - \frac{T_3}{T_1}\right) \times 100\% \quad (4)$$

where T_1 is the incident light, T_2 is the total light transmitted by the VO_2-TTWF sample, T_3 is the light scattered by the equipment, and T_4 is the light scattered by the VO_2-TTWF sample and equipment.[8] A universal test machine (MTS SANS) is used to test the mechanical properties (*e.g.* tensile stress and strain). The thermal conductivity (K) of the samples can be estimated by

$$K = \alpha\rho c \quad (5)$$

where α is the thermal diffusivity, ρ is the density, and c is the heat capacity. Knowing the thermal diffusivity, density, and heat capacity, the thermal conductivity of the VO_2-TTWF can be determined by eq 5. A light flash apparatus (LFA467 NETZSCH) and NETZSCH DSC 204 are used to obtain the thermal diffusivity and heat capacity, respectively. Lastly, the contact angle measurement is conducted by a drop shape analyzer (KRUESS GmbH DSA25S).

3. RESULTS AND DISCUSSION

3.1. Characterization of W-Doped VO_2 and Fabrication of VO_2-TTWF. XRD and DSC are performed on commercially W-doped VO_2 nanoparticles used in this study to identify the crystal structure and the transition temperature of W-doped VO_2 (Figure 1). XRD diffraction peaks of the W-doped VO_2 powder, as shown in Figure 1a, can be indexed to the monoclinic crystalline phase of VO_2.[27] The XRD pattern is in accordance with standards PDF card of JCPDS no. 65−2358,[28] and diffraction peaks from other vanadium oxide phases are not observed, confirming the purity of the nanoparticles. Figure 1b shows the transition temperature of the W-doped VO_2 by DSC measurement. The endothermic and exothermic peaks of the W-doped VO_2 powders are

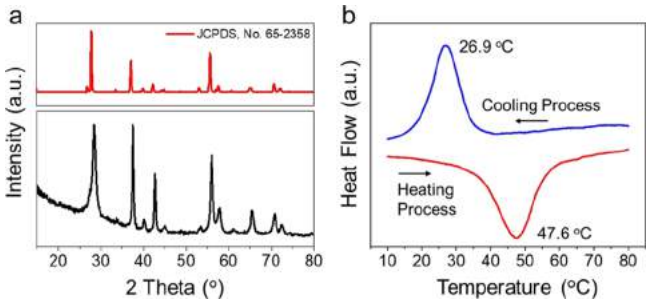

Figure 1. (a) XRD pattern of W-doped VO_2 powder and the pattern from JCPDS no. 65-2358. (b) DSC curves of W-doped VO_2 powder. The endothermic (red line) and exothermic (blue line) peaks indicate the transition temperature of W-doped VO_2 powder.

observed at 47.6 and 26.9 °C, respectively. Compared with the pure VO_2 powders, the transition temperature of W-doped VO_2 powders upon heating and cooling processes has been reduced by about 14 and 6.1 °C, respectively (Figure S1), due to W-doping. VO_2 is also a rapid response material that demonstrates a phase transition from the monoclinic insulating phase at a low temperature to the rutile metallic phase at a high temperature in only femtoseconds.[29] The lower transition temperature which is close to room temperature and the rapid phase switching time are more practical in building applications.

The fabrication process of VO_2-TTWF is illustrated in Figure 2. Balsa wood is selected as the raw material as it is a commercial timber with low density (*i.e.*, 100−250 kg m^{-3}) and is one of the fastest growing wood species in nature (*i.e.*, reaching up to 75 cm in diameter and around 20 m in height in about 5−8 years).[30] Moreover, balsa wood is easily fabricated on a large-scale by the rotary cutting method which has been widely used in the industry.[25] All these features make balsa wood a suitable material for the mass production of transparent wood. Due to the absorbance of light by lignin and the scattering effect caused by the cell walls, the original wood appears opaque.[31,32] After the delignification process, the wood becomes more porous with thinner cell walls (Figure S2) and gradually appears white in color. The morphology of the microstructure is well preserved after bleaching. However, because of the increased light reflection on the surface and the scattering in the microchannels of the bleached wood, the color of the wood becomes white and opaque at this stage.[33] To achieve the thermochromism, PVA which has a well matched refractive index (*i.e.*, ∼1.47)[34] with cellulose (∼1.525) and hemicellulose (∼1.532)[35] is selected as the polymer, and W-doped VO_2 nanoparticles are well mixed with PVA, followed by vacuum-assisted impregnation. Finally, the wood slice is polymerized at 60 °C to evaporate the water solvent in the PVA solution. The last polymerization process is the key to achieve self-densification of the wood film. Specifically, water evaporates from inside to the surface of the wood, and this phenomenon causes a negative pressure.[36] It should be noted that delignification by NaClO greatly increases the flexibility of wood cell walls; therefore, the wood structure cannot resist the compressive loads from the negative pressure, leading to collapse of the wood structures. This process significantly reduces the thickness of the wood. It can be seen from Figure 3a,b that the thickness of delignified wood has been significantly reduced by a factor of 5, that is, from 1 to 0.2 mm. In addition, a strong hydrogen bond is also formed

https://doi.org/10.1021/acsami.1c03803
ACS Appl. Mater. Interfaces XXXX, XXX, XXX−XXX

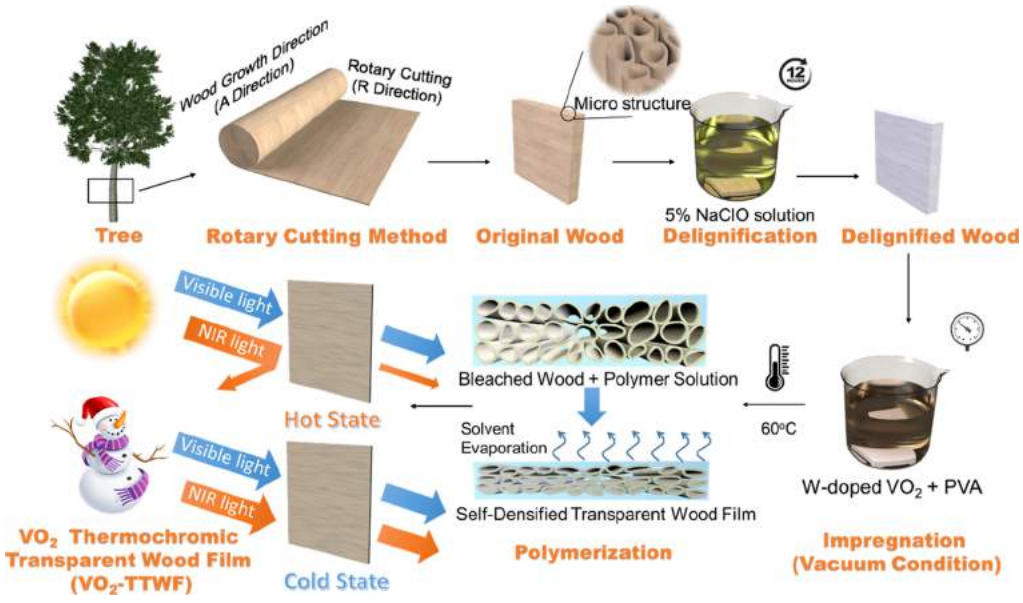

Figure 2. Fabrication process of VO_2-TTWF.

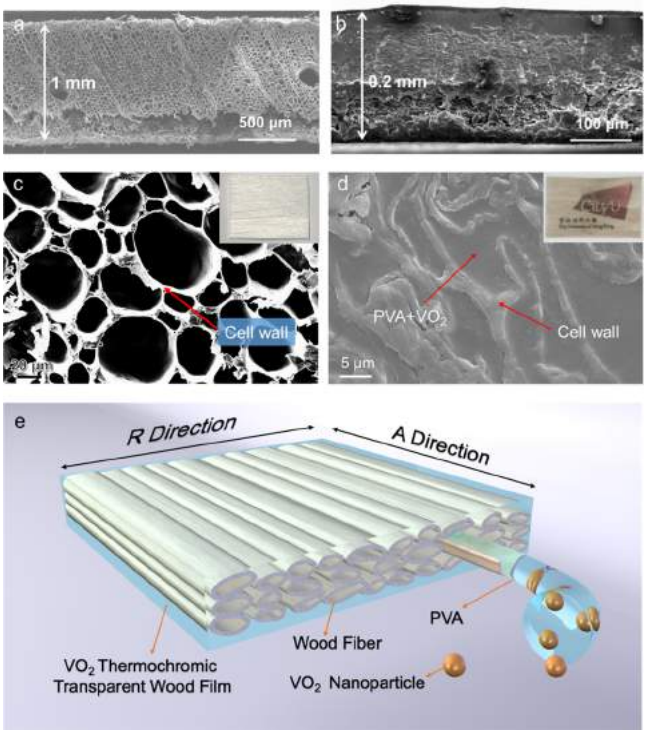

Figure 3. (a) Cross section of delignified wood. (b) Cross section of VO_2-TTWF. (c) Zoomed-in SEM image of cross section of delignified wood. (d) Zoomed-in SEM image of cross section of the VO_2-TTWF. Insets of (c,d) show the white wood and VO_2-TTWF before and after impregnation with PVA, respectively. (e) 3D schematic of internal structure of VO_2-TTWF.

between the PVA and wood cell walls, resulting in the tightly packed composite of wood and PVA. The cross-sectional SEM images shown in Figure 3c demonstrate that the microstructure of the wood is well preserved after the delignification process, and the aligned channel provides room for the infiltration of polymer. Figure 3d indicates that the microchannels of the delignified wood have been filled with the PVA (*i.e.*, containing the W-doped VO_2 nanoparticles), and the wood cell wall is closely attached with the PVA. However, it should be noted that the shape of the tubular structures of the delignified wood are deformed after polymerization due to self-densification. Overall, the self-densification effect could effectively reduce the thickness of the wood, leading to a dense VO_2-TTWF (Figure 3e).

3.2. Optical Properties of VO_2-TTWF. The unique feature of the VO_2-TTWF is the capability to passively modulate NIR transmittance with different ambient temperatures. T_{lum} and ΔT_{sol} are tunable by choosing the concentrations of W-doped VO_2 in PVA. In order to investigate the optical properties of the VO_2-TTWF, the mass concentrations of VO_2 in PVA are controlled from 1 to 6‰. The photographs of transparent wood and VO_2-TTWFs with different VO_2 concentrations are shown in Figure 4a. The pure transparent wood is colorless, meanwhile the VO_2-TTWF appears brown in color due to the presence of W-doped VO_2 nanoparticles, and the color darkens as the W-doped VO_2 concentration increases.

To characterize the thermochromism, the optical transmittance of the VO_2-TTWF was measured at the cold state and hot state, and the results are shown in Figure 4b. The VO_2-TTWF shows a remarkable optical transparency with a T_{lum} of 84.6% but without the ability to regulate light due to the absence of thermochromic VO_2 nanoparticles. The ΔT_{sol} increases while the T_{lum} decreases with the W-doped VO_2 concentration. It can been seen from Figure 4b that the VO_2-TTWF mainly tunes the NIR transmittance (*i.e.*, >700 nm), and the transmittance in the visible light region between the cold state and hot state is nearly unchanged, which is in accordance with traditional VO_2 thermochromic smart windows.[19,37] The results based on the transmittance spectra of VO_2-TTWF (Table 1) show that the average value of T_{lum} is 50.25% at the cold and hot states. Meanwhile, the ΔT_{sol} can reach 3.4% when the VO_2 content is up to 6‰; it should be noted that the T_{lum} and ΔT_{sol} of VO_2-TTWF are significantly influenced by the concentration of VO_2 particles, and the ΔT_{sol} can be further improved to ~4% when the VO_2 concentration reaches 10‰. However, the T_{lum} was reduced to only around 20% (Figure S3) which is too low for window applications, and

https://doi.org/10.1021/acsami.1c03803
ACS Appl. Mater. Interfaces XXXX, XXX, XXX−XXX

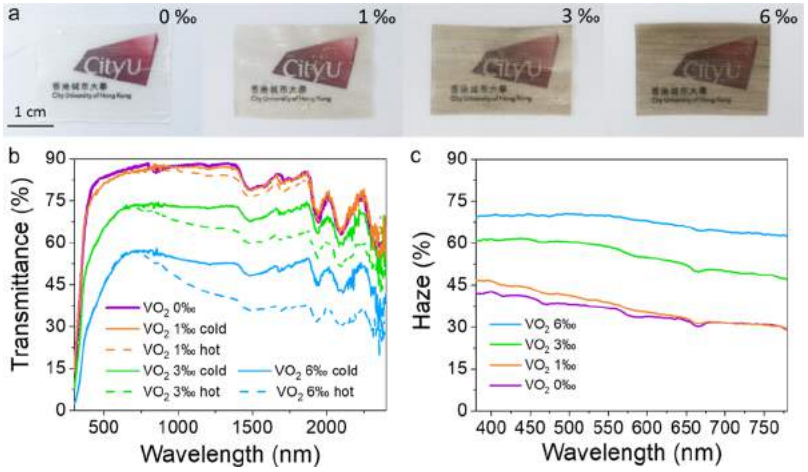

Figure 4. (a) Thermochromic transparent wood with different concentrations of W-doped VO_2 (0, 1, 3, and 6‰ from left to right); (b) temperature-dependent optical transmittance spectra of VO_2-TTWF; and (c) optical transmittance haze of VO_2-TTWF.

Table 1. T_{lum} and ΔT_{sol} Comparison of VO_2-TTWF with Different Concentrations of W-Doped VO_2 and Glass-Based VO_2 Thermochromic Smart Windows

	$T_{lum,cold}$ (%)	$T_{lum,hot}$ (%)	ΔT_{sol} (%)
VO2-TTWF 0‰	84.6 ± 0.7	84.6 ± 0.7	0.0
VO_2-TTWF 1‰	82.8 ± 0.7	82.8 ± 0.7	0.7 ± 0.1
VO_2-TTWF 3‰	68.8 ± 0.2	68.7 ± 0.3	2.7 ± 0.2
VO_2-TTWF 6‰	50.9 ± 0.5	50.1 ± 0.5	3.4 ± 0.2
glass-based W-doped VO_2 thermochromic window[42]	44.8	47.4	6.0

the color is unfavorable (*i.e.*, dark brown). Therefore, in the following tests of mechanical, thermal, and hydrophobic properties as well as the model house experiment, the 6‰-VO_2-TTWF wood is selected. The experimental results also demonstrate that VO_2 can be successfully combined with the transparent wood, and the solar radiation regulation ability of VO_2 can still be maintained. In addition, a UV aging test has also been conducted in a UV aging box (UVA340) to examine the stability of the 6‰-VO_2-TTWF under UV exposure. The test has been conducted continuously for 50 h which is equivalent to a 14-days solar exposure in Hong Kong's local climate. The results show that there is no significant change in the transmittance spectrum of the 6‰-VO_2-TTWF before and after the UV exposure (Figure S4 in the Supporting Information), proving that the VO_2-TTWF has a relatively stable optical property against the UV radiation.

Due to the collective light scattering at the interfaces of the polymer and delignified wood, the haze of the transparent wood is normally high.[6] Hu's group developed a method using NaClO in the delignification process to reduce optical haze,[7,28] and the same method is used in this study. The influence of W-doped VO_2 nanoparticles on haze is also investigated here. As shown in Figure 4c, the haze increases as the W-doped VO_2 content increases. Previous studies have proved that the VO_2 particles could lead to a significant optical dispersion, and the refractive index of VO_2 varies from 3.0 to 3.6 with the change of temperature.[38,39] The VO_2 nanoparticles enhance the light scattering, which has a detrimental effect on the refractive index matching between PVA and cellulose, leading to a

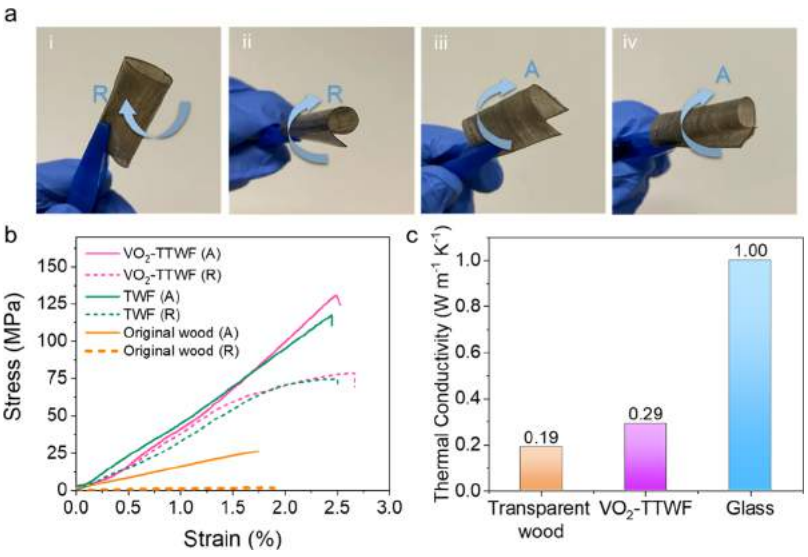

Figure 5. (a) VO_2-TTWF was folded and rolled in *A* and *R* directions. (b) Stress–strain curves of VO_2-TTWF, TWF, and original wood in *A* and *R* directions. (c) Comparison of thermal conductivity between VO_2-TTWF, transparent wood, and glass.

https://doi.org/10.1021/acsami.1c03803
ACS Appl. Mater. Interfaces XXXX, XXX, XXX−XXX

stronger scattering at the interface of the cell walls and the polymer.[40,41] This phenomenon causes increased haze with the increase of VO_2 concentration in the VO_2-TTWF.

It should be also noted that the haze of transparent wood can be further controlled by the delignification time,[7] which can be utilized to meet different user requirements (*e.g.* high haze for privacy, low haze for clear target).

3.3. Mechanical and Thermal Properties of VO_2-TTWF. VO_2-TTWF is in the form of film, which is convenient for pasting on the inner side of an existing window. As shown in Figure 5a, it can also be folded and rolled in both *A* direction (along with the direction of wood fiber, Figure 3e) and *R* direction (normal to the direction of wood fiber, Figure 3e). In addition, the density of VO_2-TTWF is 173 kg m^{-3}, which is only 0.07 times of glass (*i.e.*, 2500 kg m^{-3}). The flexibility and light weight make VO_2-TTWF easy to transport and install. Regarding its mechanical properties, the tensile stress−strain was tested and is presented in Figure 5b and Table 2. Thanks to the anisotropic properties of wood, the

Table 2. Mechanical Property Comparison between the Original Wood, Transparent Wood Film, VO_2-TTWF, and PVA

	strain, ε [%]	stress, σ [MPa]	Young's modulus, E [GPa]
original wood (*A*)	1.7 ± 0.1	26.4 ± 1.0	1.60 ± 0.10
original wood (*R*)	1.9 ± 0.1	0.7 ± 0.1	0.04 ± 0.01
transparent wood film (*A*)	2.5 ± 0.2	117.6 ± 2.8	4.70 ± 0.50
transparent wood film (*R*)	2.5 ± 0.1	74.7 ± 1.9	3.00 ± 0.10
VO_2-TTWF (*A*)	2.5 ± 0.2	130.6 ± 3.8	5.20 ± 0.42
VO_2-TTWF (*R*)	2.7 ± 0.1	78.5 ± 2.0	2.90 ± 0.21
PVA	4.2 ± 0.2	25.9 ± 4.0	0.62 ± 0.10

mechanical properties of VO_2-TTWF also demonstrate a difference in *A* and *R* directions. The tensile stress (σ) and Young's modulus (E) of the VO_2-TTWF in the *A* direction are 130.6 MPa and 5.2 GPa, respectively, which are much stronger than that of the original wood (*i.e.*, σ = 26.4 MPa and E = 1.6 GPa) and much higher than that of the previously reported VO_2 wood[14] (*i.e.*, σ = 74.57 MPa and E = 1.47 GPa). The high strength is ascribed to the dense packing of cellulose microfibrils during the self-densification as well as the effective hydrogen bonding between the cell walls and PVA.[43] It should be noted that the tensile stress of the VO_2-TTWF in the A direction is close to that of traditional soda-lime glass (*i.e.*, 165 MPa).[10] Apart from the measurement in the *A* direction, the σ and E of the VO_2-TTWF in the *R* direction are also recorded, showing a value of 78.5 MPa and 2.9 GPa, respectively. Moreover, because of the impregnation of PVA, the strain (ε) of VO_2-TTWF is improved in both *A* and *R* directions compared with the original wood (Table 2). Additionally, a transparent wood film (TWF) impregnated only with PVA is also fabricated and its mechanical properties are compared to the VO_2-TTWF. It can be seen from Table 2 that the transparent wood shows a similar mechanical strength to the VO_2-TTWF, implying that VO_2 nanoparticles have almost no significant effect on mechanical properties. Comparing with the PVA film whose σ is 25.9 MPa (Figure S5), the σ of VO_2-TTWF in both *A* and *R* directions shows higher values due to the reinforcement from wood fibers.

Wood is an excellent thermal insulation material (*i.e.*, K = 0.0381−0.0665 W m^{-1} K^{-1})[44] which is suitable for use as a building material to minimize the heat gain/loss through the building, thus improving a building's energy efficiency.[45−47] As the thermal conductivity of the wood after adding PVA and W-doped VO_2 is unknown, the thermal conductivity of the VO_2-TTWF along the perpendicular direction to the wood fibers is measured at room temperature. Laser flash apparatus (LFA) measurement is conducted to determine the thermal diffusivity of VO_2-TTWF. Next, the thermal conductivity of VO_2-TTWF is calculated using eq 5 in Section 2.4. The comparison among the thermal conductivities of several materials is illustrated in Figure 5c. The thermal conductivity of glass[7] is about 1 W m^{-1} K^{-1} which is the highest among these materials. Due to the low thermal conductivity of the cell walls and PVA, the thermal conductivity of transparent wood[25] is 0.19 W m^{-1} K^{-1}, much lower than that of glass. Adding the W-doped VO_2 nanoparticles, the thermal conductivity of VO_2-TTWF increases slightly to 0.29 W m^{-1} K^{-1}. This can be ascribed to the high thermal conductivity value of VO_2 (*i.e.*, 6.6 W m^{-1} K^{-1})[48] added to the VO_2-TTWF. When compared with glass, the thermal conductivity of VO_2-TTWF is still much lower, showing promise as an energy-efficient material for smart windows in building applications.

3.4. Self-Cleaning and Antidust Functions of VO_2-TTWF. Normally, the waterproof ability of wood is poor. As a result, oil-based paint is always painted on wood-based materials (*e.g.* furniture) to prevent rotting in a humid environment. In a previous study of transparent wood, Li *et al.* utilize the light-guiding effect of wood to develop a building material and demonstrated waterproof ability due to the usage of hydrophobic epoxy in their transparent wood.[10] Different from other polymers (such as epoxy, PMMA, *etc.*), PVA is a nontoxic and totally degradable polymer in the natural environment;[24] the key reason that we selected PVA in this work to develop a totally environment-friendly TTWF. However, PVA is a water-soluble polymer,[49] so the moisture stability of the transparent wood is not good. In addition, the surface of the wood easily accumulates dust, and if the transparent wood becomes dirty, it cannot be cleaned with a wet cloth because of the sensitivity to water. Various methods have been proposed to overcome these drawbacks, such as coating with oil or ZnO.[50] In this work, the surface of the VO_2-TTWF is treated by OTS, which is a highly transparent and stable material. Therefore, a hydrophobic transparent wood film is developed, achieving self-cleaning and antidust functions to reduce the housework load of cleaning windows. With the coating of the PVA-SiO_2 polymer composite, the surface roughness is improved,[26] and OTS reduces the surface energy, which traps a lot of air in the cavities and interfaces of the wood surface.[26] Therefore, the contact area between the wood and water droplets is small, and the wood itself is protected from wetting. A comparison of the contact angle measurement results of glass and VO_2-TTWF before and after surface treatment are exhibited in Figure 6. Traditional glass shows a small contact angle of 29.7°, meaning that traditional glass is hydrophilic without self-cleaning and antidust abilities. The VO_2-TTWF before the surface treatment demonstrates a hydrophilic property with a contact angle of 45.1° because of the polyhydroxy property of PVA. However, after the surface treatment by coating PVA-SiO_2/OTS, the contact angle of VO_2-TTWF increases to 121.9°, and the surface is transformed from hydrophilic to hydrophobic. Due to the hydrophobic

https://doi.org/10.1021/acsami.1c03803
ACS Appl. Mater. Interfaces XXXX, XXX, XXX−XXX

Figure 6. Contact angle measurement: (a) VO_2-TTWF after surface treatment by coating PVA-SiO_2/OTS, the contact angle is 121.9°; (b) VO_2-TTWF before surface treatment, the contact angle is 45.1°; and (c) glass, the contact angle is 29.7°.

property of the VO_2-TTWF, the waterproof ability is significantly improved, and dust particles are hard to accumulate on the surface,[51] eventually achieving self-cleaning and antidust functions. Video S1 demonstrates the waterproof ability and antidust performance of VO_2 TTWF before and after coating with OTS. It can be clearly seen that the water and dust can be more easily removed after the hydrophobic treatment for VO_2-TTWF. The optical properties of VO_2-TTWF have also been characterized after coating with the OTS. The results show that the $T_{lum,cold}$ and $T_{lum,hot}$ are 46.4 and 45.7%, respectively, resulting in ΔT_{sol} of 3.5%. This proves that the hydrophobic treatment does not affect the optical performance of VO_2-TTWF significantly (*i.e.*, $T_{lum,cold}$ = 50.9%, $T_{lum,hot}$ = 50.1% and ΔT_{sol} = 3.4% without coating the OTS). In addition, the mechanical strength is 116.3 MPa in the A direction and 62.1 MPa in the *R* direction after coating with the OTS (130.6 MPa in *A* direction and 78.5 MPa in the *R* direction before coating with the OTS). For strain, it slightly varied from 2.5 to 2.1% in the A direction and from 2.5 to 2.4% in the *R* direction. Overall, the VO_2-TTWF can still maintain a strong mechanical performance even after coating with the OTS, showing the effective practicability of this method for the surface hydrophobic treatment.

3.5. Model House Experiment. To evaluate the energy-saving performance of VO_2-TTWF, an experiment using model houses was conducted. A large-scale VO_2-TTWF (10 cm × 10 cm) was directly pasted on the inner face of a glass window and installed in an acrylic model house with the dimensions of 20 cm × 20 cm × 20 cm (Figure 7a, model house 1). Another model house, model house 2, was set as the reference having only a bare glass window installed. Due to the solar regulation ability in the NIR region, these two model houses were placed under an IR lamp to monitor their indoor air temperature and window temperature to compare the heat-shielding ability of the VO_2-TTWF and the bare glass panel. As shown in Figure 7b, with continuous exposure under the IR light, the indoor air temperature of both model houses increased sharply. Notably, the indoor air temperature of model house 2 increased to 72.1 °C from 25.5 °C. However, the indoor air temperature increase of model house 1 was relatively small, increasing by about 12.4 °C, from 25.8 to 38.2 °C. Clearly, VO_2-TTWF demonstrated a good heat shielding ability; hence, the indoor air temperature of model house 1 can be controlled at a relatively low level. When the IR lamp was turned off, the indoor air temperature of model house 2 was 33.9 °C higher than that of model house 1, and the indoor air temperature of model house 2 decreased quickly to its initial indoor air temperature (~25.5 °C) in 2 min. However, the indoor air temperature of model house 1 took around 5 min to return to its initial temperature. The key reason for this phenomenon is attributed to the large heat capacity of VO_2-TTWF over bare glass. Figure 7c exhibits the window temperature of the two model houses. Due to the strong NIR absorption of VO_2, the temperature of VO_2-TTWF increased dramatically; it was 12 °C higher than that of the normal glass at the moment of turning off the IR light. Because of the slow heat dissipation of VO_2-TTWF after turning off the light, the indoor air temperature reduction of model house 1 was not as significant as model house 2. From Figure 7c, it can be seen that the heating and cooling rates of VO_2-TTWF are both slower than that of normal glass, indirect evidence that the heat capacity of VO_2-TTWF is greater than that of glass. Based on our measurement, the results in Figure 7d show that the heat capacity of glass is around 1 J g^{-1} $°C^{-1}$, but the heat capacity of VO_2-TTWF is higher than that of glass, increasing with the temperature from 1.5 to 4.5 J g^{-1} $°C^{-1}$. The relatively high heat capacity can store more thermal energy to reduce

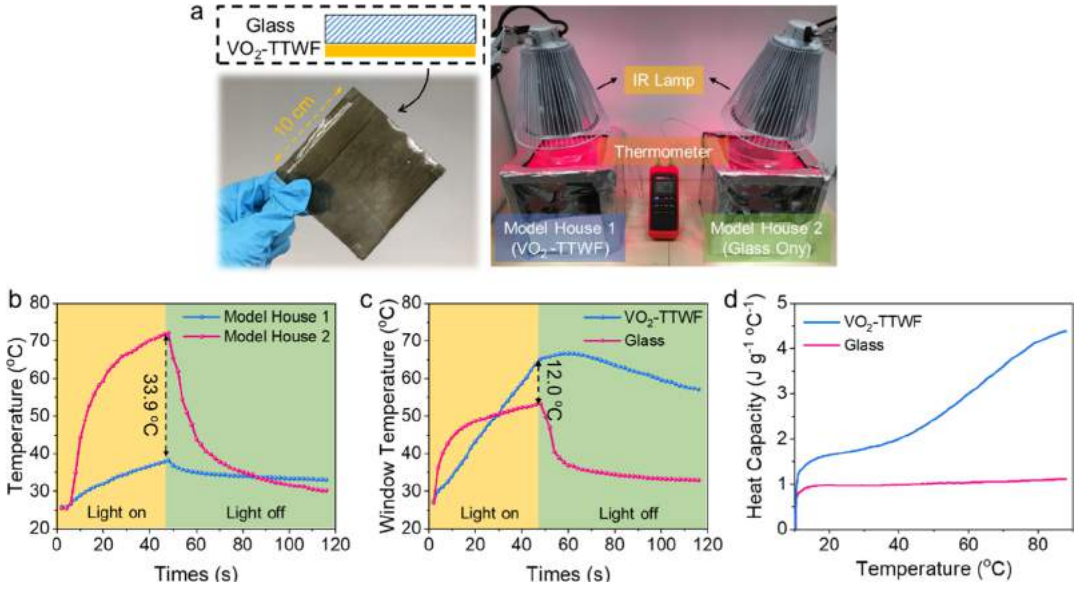

Figure 7. (a) Photo of VO_2-TTWF pasted on the glass and the experimental set up for the model house test; (b) time-dependence of indoor air-temperature profile in model house 1 with VO_2-TTWF and model house 2 with pure glass; (c) window temperature of VO_2-TTWF pasted on the glass in model house 1 and the normal glass in model house 2; (d) temperature-dependent-heat capacities of VO_2-TTWF and normal glass.

https://doi.org/10.1021/acsami.1c03803
ACS Appl. Mater. Interfaces XXXX, XXX, XXX−XXX

Table 3. Comparison of Various Energy-Efficient Transparent Wood (TW)

							model house test			
	type	scale (mm)	T_{lum} (%)	ΔT_{sol} (%)	σ (MPa)	E (GPa)	$T_{glass} - T_{wood}$ (°C)	K (W m^{-1} K^{-1})	self-cleaning	references
Cs_xWO_3-TW	bulk	60 × 30 × 5	52.4		59.80	2.72	5.2		no	13
ATO-TW	bulk	50 × 50 × 1	50.9		113.06	4.27	6.5	0.20	no	58
VO_2-TW	bulk	25 × 25 × 2.5	50.2		74.57	1.47	25.7	0.20	no	14
VO_2-TTWF	film	100 × 100 × 0.2	50.5	3.4	130.60	5.20	33.9	0.29	yes	this work

cooling/heating loads and shift energy load to low price periods.[52] The model house experiment demonstrates that VO_2-TTWF shows an excellent heat shielding ability and has potential to be applied as energy-efficient materials on smart windows.

3.6. Comparison with Other Studies. Table 3 lists the typical energy-efficient transparent wood that has been reported very recently. It can be seen that other studies focus on the bulk wood, aiming at replacing traditional windows. However, for the first time, an energy-efficient wood film has been developed in this study to directly attach on an existing window; thus, the installation and maintenance cost can be significantly reduced, simultaneously avoiding the weather resistance problem of wood, thereby extending the life span and making it easy to adopt in real applications. For the optical properties, the visible transparency of all the samples is similar, but VO_2-TTWF demonstrates different NIR transmittance between cold and hot states, resulting in the ΔT_{sol} of 3.4%. For the mechanical properties, even though VO_2-TTWF is a thin film, it exhibits the highest σ and E due to the self-densification leading to a dense and robust composite. In addition, a large scale VO_2-TTWF (100 mm × 100 mm) was used to conduct the model house test, and the temperature difference between wood window and glass window ($T_{glass} - T_{wood}$) proves that the energy saving potential of VO_2-TTWF is also significant compared with other studies. The self-cleaning and antidust functions as well as the waterproof ability were also developed for the VO_2-TTWF by coating the OTS, making it more practical for real applications. In summary, the VO_2-TTWF demonstrates great potential as a green and energy-efficient building material. It should also be noted that, inspired by the VO_2-TTWF, other nanoparticles, such as ZnO, CeO_2, TiO_2, and Cr_2O_3[39,53−57] are also potential candidates to be integrated with wood to develop various multifunctional and environment-friendly wood film for use in gas sensing, optoelectronic devices, antibacterial applications, and photocatalysis, greatly expanding the applications of wood films.

4. CONCLUSIONS

In this study, a VO_2 thermochromic transparent wood film (VO_2-TTWF) is developed. The wood film is optically transparent with T_{lum} of 50.5%, achieving intelligent dynamic solar irradiance regulation ability (*i.e.*, ΔT_{sol} = 3.4%). The tensile strength of the VO_2-TTWF is also recorded at about 130.6 MPa along the A direction, demonstrating a robust mechanical property. Moreover, VO_2-TTWF inherits the excellent thermal insulation characteristics of wood and exhibits a low thermal conductivity of 0.29 W m^{-1} K^{-1} along the direction perpendicular to the wood fibers. Furthermore, the surface of VO_2-TTW is modified to achieve hydrophobic self-cleaning and antidust functions. Most importantly, the VO_2-TTWF is thin, making it convenient to paste on the inner face of existing windows, which significantly reduces the installation cost. The model house experiment proves that VO_2-TTWF can significantly reduce the indoor air temperature compared with a bare glass window because of the NIR shielding ability of VO_2. Additionally, the wood-PVA composite makes the VO_2-TTWF become a totally sustainable and recyclable environmentally friendly material. These unique features render the VO_2-TTWF with great potential to be developed as a new generation energy-efficient material, which can be widely applied on smart windows.

■ ASSOCIATED CONTENT

Supporting Information

The Supporting Information is available free of charge at https://pubs.acs.org/doi/10.1021/acsami.1c03803.

DSC curves of VO_2 powder; cross-sectional SEM images of balsa wood; photo and transmittance spectrum of 10‰ W-doped VO_2-TTWF; transmittance spectrum of VO_2-TTWF before and after the UV aging test; and stress−strain curve of PVA (PDF)

Waterproof and antidust demonstration of VO_2 thermochromic transparent wood film (MP4)

■ AUTHOR INFORMATION

Corresponding Author

Chi Yan Tso − *School of Energy and Environment, City University of Hong Kong, Kowloon Tong, Hong Kong, China*; orcid.org/0000-0002-7725-2172; Email: chiytso@cityu.edu.hk

Authors

Sai Liu − *School of Energy and Environment, City University of Hong Kong, Kowloon Tong, Hong Kong, China*

Hau Him Lee − *School of Energy and Environment, City University of Hong Kong, Kowloon Tong, Hong Kong, China*

Yu Wei Du − *School of Energy and Environment, City University of Hong Kong, Kowloon Tong, Hong Kong, China*

Kin Man Yu − *Department of Physics, City University of Hong Kong, Kowloon Tong, Hong Kong, China*

Shien-Ping Feng − *Department of Mechanical Engineering, The University of Hong Kong, Pokfulam, Hong Kong, China*; orcid.org/0000-0002-3941-1363

Baoling Huang − *Department of Mechanical and Aerospace Engineering, The Hong Kong University of Science and Technology, Kowloon, Hong Kong, China*; orcid.org/0000-0001-7507-5371

Complete contact information is available at: https://pubs.acs.org/10.1021/acsami.1c03803

Author Contributions

S.L. and C.Y.T. proposed the concept and designed the methodology. S.L. and Y.W.D. conducted the experiment. S.L., H.H.L., and Y.W.D. finished the first draft. K.M.Y., S.P.F., B.L.H., and C.Y.T. reviewed and edited the manuscript. C.Y.T. acquired the funding and supervised the whole project.

https://doi.org/10.1021/acsami.1c03803
ACS Appl. Mater. Interfaces XXXX, XXX, XXX−XXX

Notes

The authors declare no competing financial interest.

■ ACKNOWLEDGMENTS

C.Y.T. received funding from Hong Kong Research Grant Council (RGC) *via* Collaborative Research Fund (CRF) account C6022-16G and General Research Fund (GRF) account 16200518 and City University of Hong Kong StartUp Fund account 9610411. There are no competing interests to declare.

■ REFERENCES

(1) Chen, C.; Kuang, Y.; Zhu, S.; Burgert, I.; Keplinger, T.; Gong, A.; Li, T.; Berglund, L.; Eichhorn, S. J.; Hu, L. Structure−Property−Function Relationships of Natural and Engineered Wood. *Nat. Rev. Mater.* **2020**, *5*, 642−666.

(2) Fu, Q.; Chen, Y.; Sorieul, M. Wood-Based Flexible Electronics. *ACS Nano* **2020**, *14*, 3528−3538.

(3) Kong, W.; Wang, C.; Jia, C.; Kuang, Y.; Pastel, G.; Chen, C.; Chen, G.; He, S.; Huang, H.; Zhang, J.; Wang, S.; Hu, L. Muscle-Inspired Highly Anisotropic, Strong, Ion-Conductive Hydrogels. *Adv. Mater.* **2018**, *30*, 1801934.

(4) Li, T.; Zhai, Y.; He, S.; Gan, W.; Wei, Z.; Heidarinejad, M.; Dalgo, D.; Mi, R.; Zhao, X.; Song, J.; Dai, J.; Chen, C.; Aili, A.; Vellore, A.; Martini, A.; Yang, R.; Srebric, J.; Yin, X.; Hu, L. A Radiative Cooling Structural Material. *Science* **2019**, *364*, 760−763.

(5) Yang, H.; Wang, Y.; Yu, Q.; Cao, G.; Yang, R.; Ke, J.; Di, X.; Liu, F.; Zhang, W.; Wang, C. Composite Phase Change Materials with Good Reversible Thermochromic Ability in Delignified Wood Substrate for Thermal Energy Storage. *Appl. Energy* **2018**, *212*, 455−464.

(6) Zhu, M.; Song, J.; Li, T.; Gong, A.; Wang, Y.; Dai, J.; Yao, Y.; Luo, W.; Henderson, D.; Hu, L. Highly Anisotropic, Highly Transparent Wood Composites. *Adv. Mater.* **2016**, *28*, 5181−5187.

(7) Jia, C.; Chen, C.; Mi, R.; Li, T.; Dai, J.; Yang, Z.; Pei, Y.; He, S.; Bian, H.; Jang, S.-H.; Zhu, J. Y.; Yang, B.; Hu, L. Clear Wood toward High-Performance Building Materials. *ACS Nano* **2019**, *13*, 9993−10001.

(8) Li, Y.; Fu, Q.; Yu, S.; Yan, M.; Berglund, L. Optically Transparent Wood from a Nanoporous Cellulosic Template: Combining Functional and Structural Performance. *Biomacromolecules* **2016**, *17*, 1358−1364.

(9) Zhu, M.; Li, T.; Davis, C. S.; Yao, Y.; Dai, J.; Wang, Y.; AlQatari, F.; Gilman, J. W.; Hu, L. Transparent and Haze Wood Composites for Highly Efficient Broadband Light Management in Solar Cells. *Nano Energy* **2016**, *26*, 332−339.

(10) Li, T.; Zhu, M.; Yang, Z.; Song, J.; Dai, J.; Yao, Y.; Luo, W.; Pastel, G.; Yang, B.; Hu, L. Wood Composite as an Energy Efficient Building Material: Guided Sunlight Transmittance and Effective Thermal Insulation. *Adv. Energy Mater.* **2016**, *6*, 1601122.

(11) Li, Y.; Vasileva, E.; Sychugov, I.; Popov, S.; Berglund, L. Optically Transparent Wood: Recent Progress, Opportunities, and Challenges. *Adv. Opt. Mater.* **2018**, *6*, 1800059.

(12) Liu, Z. National Carbon Emissions from the Industry Process: Production of Glass, Soda Ash, Ammonia, Calcium Carbide and Alumina. *Appl. Energy* **2016**, *166*, 239−244.

(13) Yu, Z.; Yao, Y.; Yao, J.; Zhang, L.; Chen, Z.; Gao, Y.; Luo, H. Transparent Wood Containing CsXWO3 Nanoparticles for Heat-Shielding Window Applications. *J. Mater. Chem. A* **2017**, *5*, 6019−6024.

(14) Zhang, L.; Wang, A.; Zhu, T.; Chen, Z.; Wu, Y.; Gao, Y. Transparent Wood Composites Fabricated by Impregnation of Epoxy Resin and W-Doped VO2 Nanoparticles for Application in Energy-Saving Windows. *ACS Appl. Mater. Interfaces* **2020**, *12*, 34777−34783.

(15) Lang, A. W.; Li, Y.; De Keersmaecker, M.; Shen, D. E.; Österholm, A. M.; Berglund, L.; Reynolds, J. R. Transparent Wood Smart Windows: Polymer Electrochromic Devices Based on Poly(3,4-Ethylenedioxythiophene):Poly(Styrene Sulfonate) Electrodes. *ChemSusChem* **2018**, *11*, 854−863.

(16) Wang, L.; Liu, Y.; Zhan, X.; Luo, D.; Sun, X. Photochromic Transparent Wood for Photo-Switchable Smart Window Applications. *J. Mater. Chem. C* **2019**, *7*, 8649−8654.

(17) Zhou, Y.; Dong, X.; Mi, Y.; Fan, F.; Xu, Q.; Zhao, H.; Wang, S.; Long, Y. Hydrogel Smart Windows. *J. Mater. Chem. A* **2020**, *8*, 10007−10025.

(18) Zhang, Y.; Tso, C. Y.; Iñigo, J. S.; Liu, S.; Miyazaki, H.; Chao, C. Y. H.; Yu, K. M. Perovskite Thermochromic Smart Window: Advanced Optical Properties and Low Transition Temperature. *Appl. Energy* **2019**, *254*, 113690.

(19) Xu, F.; Cao, X.; Luo, H.; Jin, P. Recent Advances in VO2-Based Thermochromic Composites for Smart Windows. *J. Mater. Chem. C* **2018**, *6*, 1903−1919.

(20) Cui, Y.; Ke, Y.; Liu, C.; Chen, Z.; Wang, N.; Zhang, L.; Zhou, Y.; Wang, S.; Gao, Y.; Long, Y. Thermochromic VO2 for Energy-Efficient Smart Windows. *Joule* **2018**, *2*, 1707−1746.

(21) Liu, S.; Tso, C. Y.; Lee, H. H.; Zhang, Y.; Yu, K. M.; Chao, C. Y. H. Bio-Inspired TiO2 Nano-Cone Antireflection Layer for the Optical Performance Improvement of VO2 Thermochromic Smart Windows. *Sci. Rep.* **2020**, *10*, 11376.

(22) Kong, M.; Egbo, K.; Liu, C. P.; Hossain, M. K.; Tso, C. Y.; Hang Chao, C. Y.; Yu, K. M. Rapid Thermal Annealing Assisted Facile Solution Method for Tungsten-Doped Vanadium Dioxide Thin Films on Glass Substrate. *J. Alloys Compd.* **2020**, *833*, 155053.

(23) Madida, I. G.; Simo, A.; Sone, B.; Maity, A.; Kana Kana, J. B.; Gibaud, A.; Merad, G.; Thema, F. T.; Maaza, M. Submicronic VO2-PVP Composites Coatings for Smart Windows Applications and Solar Heat Management. *Sol. Energy* **2014**, *107*, 758−769.

(24) Ben Halima, N. Poly(Vinyl Alcohol): Review of Its Promising Applications and Insights into Biodegradation. *RSC Advances* **2016**, *6*, 39823−39832.

(25) Mi, R.; Li, T.; Dalgo, D.; Chen, C.; Kuang, Y.; He, S.; Zhao, X.; Xie, W.; Gan, W.; Zhu, J.; Srebric, J.; Yang, R.; Hu, L. A Clear, Strong, and Thermally Insulated Transparent Wood for Energy Efficient Windows. *Adv. Funct. Mater.* **2020**, *30*, 1907511.

(26) Liu, F.; Wang, S.; Zhang, M.; Ma, M.; Wang, C.; Li, J. Improvement of Mechanical Robustness of the Superhydrophobic Wood Surface by Coating PVA/SiO 2 Composite Polymer. *Appl. Surf. Sci.* **2013**, *280*, 686−692.

(27) Hou, J.; Zhang, J.; Wang, Z.; Zhang, Z.; Ding, Z. The Phase Transition of W-Doped VO2 Nanoparticles Synthesized by an Improved Thermolysis Method. *J. Nanosci. Nanotechnol.* **2013**, *13*, 1543−1548.

(28) Li, X.; Zhang, S.; Yang, L.; Li, X.; Chen, J.; Huang, C. A Convenient Way to Reduce the Hysteresis Width of VO2(M) Nanomaterials. *New J. Chem.* **2017**, *41*, 15260−15267.

(29) Yu, S.; Wang, S.; Lu, M.; Zuo, L. A Metal-Insulator Transition Study of VO2 Thin Films Grown on Sapphire Substrates. *J. Appl. Phys.* **2017**, *122*, 235102.

(30) Borrega, M.; Ahvenainen, P.; Serimaa, R.; Gibson, L. Composition and Structure of Balsa (Ochroma Pyramidale) Wood. *Wood Sci. Technol.* **2015**, *49*, 403−420.

(31) Wu, Y.; Wu, J.; Yang, F.; Tang, C.; Huang, Q. Effect of H2O2 Bleaching Treatment on the Properties of Finished Transparent Wood. *Polymers (Basel)* **2019**, *11*, 776.

(32) Li, H.; Guo, X.; He, Y.; Zheng, R. House Model with 2−5 Cm Thick Translucent Wood Walls and Its Indoor Light Performance. *Eur. J. Wood Wood Prod.* **2019**, *77*, 843−851.

(33) Li, Y.; Fu, Q.; Yang, X.; Berglund, L. Transparent Wood for Functional and Structural Applications. *Philos. Trans. R. Soc., A* **2018**, *376*, 20170182.

(34) Schnepf, M. J.; Mayer, M.; Kuttner, C.; Tebbe, M.; Wolf, D.; Dulle, M.; Altantzis, T.; Formanek, P.; Förster, S.; Bals, S.; König, T. A. F.; Fery, A. Nanorattles with Tailored Electric Field Enhancement. *Nanoscale* **2017**, *9*, 9376−9385.

https://doi.org/10.1021/acsami.1c03803
ACS Appl. Mater. Interfaces XXXX, XXX, XXX−XXX

(35) Fink, S. Transparent Wood−A New Approach in the Functional Study of Wood Structure. *Holzforschung* **1992**, *46*, 403−408.
(36) Li, K.; Wang, S.; Chen, H.; Yang, X.; Berglund, L. A.; Zhou, Q. Self-Densification of Highly Mesoporous Wood Structure into a Strong and Transparent Film. *Adv. Mater.* **2020**, *32*, 2003653.
(37) Chang, T.; Cao, X.; Long, Y.; Luo, H.; Jin, P. How to Properly Evaluate and Compare the Thermochromic Performance of VO2-Based Smart Coatings. *J. Mater. Chem. A* **2019**, *7*, 24164−24172.
(38) Kana, K. J. B.; Ndjaka, J. M.; Vignaud, G.; Gibaud, A.; Maaza, M. Thermally Tunable Optical Constants of Vanadium Dioxide Thin Films Measured by Spectroscopic Ellipsometry. *Opt. Commun.* **2011**, *284*, 807−812.
(39) Maaza, M.; Hamidi, D.; Simo, A.; Kerdja, T.; Chaudhary, A. K.; Kana Kana, J. B. Optical limiting in pulsed laser deposited VO2 nanostructures. *Opt. Commun.* **2012**, *285*, 1190−1193.
(40) Laaksonen, K.; Li, S.-Y.; Puisto, S. R.; Rostedt, N. K. J.; Ala-Nissila, T.; Granqvist, C. G.; Nieminen, R. M.; Niklasson, G. A. Nanoparticles of TiO2 and VO2 in Dielectric Media: Conditions for Low Optical Scattering, and Comparison between Effective Medium and Four-Flux Theories. *Sol. Energy Mater. Sol. Cells* **2014**, *130*, 132−137.
(41) Chen, H.; Baitenov, A.; Li, Y.; Vasileva, E.; Popov, S.; Sychugov, I.; Yan, M.; Berglund, L. Thickness Dependence of Optical Transmittance of Transparent Wood: Chemical Modification Effects. *ACS Appl. Mater. Interfaces* **2019**, *11*, 35451−35457.
(42) Hu, L.; Tao, H.; Chen, G.; Pan, R.; Wan, M.; Xiong, D.; Zhao, X. Porous W-Doped VO2 Films with Simultaneously Enhanced Visible Transparency and Thermochromic Properties. *J. Sol-Gel Sci. Technol.* **2016**, *77*, 85−93.
(43) Chen, N.-x.; Zhang, J.-h. The Role of Hydrogen-Bonding Interaction in Poly(Vinyl Alcohol)/Poly(Acrylic Acid) Blending Solutions and Their Films. *Chinese J. Polym. Sci. (English Ed.* **2010**, *28*, 903−911.
(44) Kotlarewski, N. J.; Ozarska, B.; Gusamo, B. K. *Balsa Thermal Conductivity*, 2014; Vol. *9*.
(45) Cetiner, I.; Shea, A. D. Wood Waste as an Alternative Thermal Insulation for Buildings. *Energy Build* **2018**, *168*, 374−384.
(46) Agoudjil, B.; Benchabane, A.; Boudenne, A.; Ibos, L.; Fois, M. Renewable Materials to Reduce Building Heat Loss: Characterization of Date Palm Wood. *Energy Build* **2011**, *43*, 491−497.
(47) Wang, J. S.; Demartino, C.; Xiao, Y.; Li, Y. Y. Thermal Insulation Performance of Bamboo- and Wood-Based Shear Walls in Light-Frame Buildings. *Energy Build* **2018**, *168*, 167−179.
(48) Li, R.; Ji, S.; Li, Y.; Gao, Y.; Luo, H.; Jin, P. Synthesis and Characterization of Plate-like VO2(M)@SiO 2 Nanoparticles and Their Application to Smart Window. *Mater. Lett.* **2013**, *110*, 241−244.
(49) Xu, F.; Zhang, H.; Jin, L.; Li, Y.; Li, J.; Gan, G.; Wei, M.; Li, M.; Liao, Y. Controllably Degradable Transient Electronic Antennas Based on Water-Soluble PVA/TiO2 Films. *J. Mater. Sci.* **2018**, *53*, 2638−2647.
(50) Maaza, M.; Ngom, B. D.; Achouri, M.; Manikandan, K. Functional Nanostructured Oxides. *Vacuum* **2015**, *114*, 172−187.
(51) Maharjan, S.; Liao, K.-S.; Wang, A. J.; Barton, K.; Haldar, A.; Alley, N. J.; Byrne, H. J.; Curran, S. A. Self-Cleaning Hydrophobic Nanocoating on Glass: A Scalable Manufacturing Process. *Mater. Chem. Phys* **2020**, *239*, 122000.
(52) Zhou, Y.; Wang, S.; Peng, J.; Tan, Y.; Li, C.; Boey, F. Y. C.; Long, Y. Liquid Thermo-Responsive Smart Window Derived from Hydrogel. *Joule* **2020**, *4*, 2458−2474.
(53) Sone, B. T.; Manikandan, E.; Gurib-Fakim, A.; Maaza, M. Single-Phase α-Cr2O3nanoparticles' Green Synthesis Using Callistemon Viminalis' Red Flower Extract. *Green Chem. Lett. Rev.* **2016**, *9*, 85−90.
(54) Nwanya, A. C.; Deshmukh, P. R.; Osuji, R. U.; Maaza, M.; Lokhande, C. D.; Ezema, F. I. Synthesis, Characterization and Gas-Sensing Properties of SILAR Deposited ZnO-CdO Nano-Composite Thin Film. *Sensors Actuators, B Chem.* **2015**, *206*, 671−678.
(55) Thomas, B.; Vithiya, B. S. M.; Prasad, T. A. A.; Mohamed, S. B.; Magdalane, C. M.; Kaviyarasu, K.; Maaza, M. Antioxidant and Photocatalytic Activity of Aqueous Leaf Extract Mediated Green Synthesis of Silver Nanoparticles Using Passiflora Edulis f. Flavicarpa. *J. Nanosci. Nanotechnol.* **2019**, *19*, 2640−2648.
(56) Aisida, S. O.; Madubuonu, N.; Alnasir, M. H.; Ahmad, I.; Botha, S.; Maaza, M.; Ezema, F. I. Biogenic Synthesis of Iron Oxide Nanorods Using Moringa Oleifera Leaf Extract for Antibacterial Applications. *Appl. Nanosci.* **2020**, *10*, 305−315.
(57) Magdalane, C. M.; Kaviyarasu, K.; Priyadharsini, G. M. A.; Bashir, A. K. H.; Mayedwa, N.; Matinise, N.; Isaev, A. B.; Abdullah Al-Dhabi, N.; Arasu, M. V.; Arokiyaraj, S.; Kennedy, J.; Maaza, M. Improved Photocatalytic Decomposition of Aqueous Rhodamine-B by Solar Light Illuminated Hierarchical Yttria Nanosphere Decorated Ceria Nanorods. *J. Mater. Res. Technol.* **2019**, *8*, 2898−2909.
(58) Qiu, Z.; Xiao, Z.; Gao, L.; Li, J.; Wang, H.; Wang, Y.; Xie, Y. Transparent Wood Bearing a Shielding Effect to Infrared Heat and Ultraviolet via Incorporation of Modified Antimony-Doped Tin Oxide Nanoparticles. *Compos. Sci. Technol.* **2019**, *172*, 43−48.

https://doi.org/10.1021/acsami.1c03803
ACS Appl. Mater. Interfaces XXXX, XXX, XXX−XXX